

# Adsorption Behavior and Dilational Rheology of the Cationic Alkyl Trimethylammonium Bromides at the Water/Air Interface

C. Stubenrauch,<sup>\*,†</sup> V. B. Fainerman,<sup>‡</sup> E. V. Aksenenko,<sup>§</sup> and R. Miller<sup>||</sup>

*Institut für Physikalische Chemie, Universität zu Köln, Luxemburger Str. 116, D-50939 Köln, Germany, Donetsk Medical University, 16 Ilych Avenue, Donetsk 83003, Ukraine, Institute of Colloid and Water Chemistry, 42 Vernadsky av., Kiev 252680, Ukraine, and MPI für Kolloid- und Grenzflächenforschung, D-14424 Golm, Germany*

Received: August 3, 2004

The dynamic and equilibrium surface tensions of  $C_n$ TAB solutions for  $n = 12, 14$ , and  $16$  are studied using ring and bubble pressure tensiometry. Together with respective literature values, including neutron reflectivity and dilational surface rheology measurements, the experimental data are analyzed on the basis of two theoretical models, the Frumkin model and a modified reorientation model that takes into account an intrinsic compressibility of adsorbed surfactant molecules. It turns out that this new reorientation model, earlier applied to nonionic surfactant adsorption layers, is also applicable to ionic surfactants and superior to the Frumkin isotherm. All adsorption properties of one particular surfactant can be described by a single set of model parameters.

## 1. Introduction

In the past, the adsorption and rheological behavior of the cationic alkyl trimethylammonium bromides ( $C_n$ TAB) at the solution/air interface has been studied extensively by various methods. The equilibrium surface tension of aqueous  $C_n$ TAB solutions for  $n = 10, 12, 14$ , and  $16$  was studied in refs 1–5, while in refs 6–8 the dynamic surface tensions and adsorption in the short-time range (oscillating jet and inclined plate methods) were presented, and the adsorption mechanism of  $C_n$ TAB was analyzed. In addition, experimental studies employing the neutron reflection method were published.<sup>3,9–12</sup> These studies not only provided some insight into the structure of the adsorption layer and the localization of the surface-active ion and counterions, but they also enabled one to determine the  $C_n$ TAB adsorption at the solution/air interface. The rheological behavior of adsorbed  $C_n$ TAB layers at high-surface oscillation frequencies was studied in refs 5 and 13. Moreover, an analysis of the  $C_n$ TAB adsorption layer structure was performed using sum-frequency spectroscopy.<sup>14,15</sup>

The various studies briefly summarized above provide an excellent pool of data suitable to derive a molecular model that describes all findings with a single set of model parameters. We know that the Frumkin model is capable of representing the equilibrium tensiometric data, and it agrees rather well with the values obtained by neutron reflection. However, the rheological behavior resulting from this model largely disagrees with the experimental data. Recent theoretical models assume a reorientation of adsorbed surfactant molecules (so-called intrinsic molecular compressibility) and agree very well with the

experimentally observed dependence of the limiting elasticity for various nonionic surfactants on the bulk concentration.<sup>16–19</sup>

In the present work, the experimental studies of equilibrium and dynamic tensiometry (from 1 ms to 100 s, where only few investigations were performed until now) of aqueous  $C_n$ TAB solutions are presented, and the attempt is made to generalize all known experimental data on a new theoretical basis. This theoretical description is based on quite a rigorous thermodynamic model<sup>20</sup> which assumes intrinsic compressibility of the surfactant molecules in the adsorption layer and accounts for the nonideality of the surface layer enthalpy and entropy.

## 2. Theoretical Models

In the framework of an electroneutral surface layer model, arranged by a certain choice of the Gibbs dividing surface, the equation of state of the surface layer and the adsorption isotherm for the Frumkin model for ionic surfactants are<sup>21</sup>

$$\Pi = -\frac{2RT}{\omega}[\ln(1 - \theta) + a\theta^2] \quad (1)$$

$$b[c(c + c_2)]^{1/2}f = \frac{\theta}{1 - \theta} \exp(-2a\theta) \quad (2)$$

Here,  $R$  is the gas law constant,  $T$  is the temperature,  $\Pi$  is the surface pressure ( $\Pi = \gamma_0 - \gamma$ ),  $\gamma$  and  $\gamma_0$  are the surface tensions of the solution and the solvent, respectively,  $\omega$  is the partial molar area of the ionic surfactant (about two times larger than the molar area of the solvent),  $f$  is the average activity coefficient of ions in the bulk solution,  $c$  is the ionic surfactant concentration,  $c_2$  is the inorganic (1:1) salt concentration,  $\theta = \Gamma\omega$  is the surface layer coverage by the surfactant,  $\Gamma$  is the surfactant adsorption,  $a$  is the intermolecular interaction constant, and  $b$  is the adsorption equilibrium constant.

The Debye–Hückel equation corrected for short-range interactions accurately represents the values of the average activity coefficient  $f$ :

\* Corresponding author. Present address: Department of Chemical and Biochemical Engineering, University College Dublin, Belfield, Dublin 4, Ireland. E-mail: cosima.stubenrauch@ucd.ie. Fax: +353-1-716-1177. Phone: +353-1-716-1923.

<sup>†</sup> Universität zu Köln.

<sup>‡</sup> Donetsk Medical University.

<sup>§</sup> Institute of Colloid and Water Chemistry.

<sup>||</sup> MPI für Kolloid- und Grenzflächenforschung.

$$\log f = -\frac{0.5115 \sqrt{I}}{1 + 1.316 \sqrt{I}} + 0.055 I \quad (3)$$

where  $I = c + c_2$  is the ionic strength expressed in mol l<sup>-1</sup> and the numerical constants correspond to 25 °C.<sup>22</sup>

In the model of ionized monolayers, the mutual repulsion of long-chain surfactant ions results in an additional surface pressure  $\Pi_{\text{el}}$  calculated according to the Gouy–Chapman theory for the formation of a diffuse electric double layer and with counterion binding in the Stern–Helmholtz layer adjacent to the surfactant monolayer. Neglecting counterion binding in the Stern–Helmholtz layer, one obtains an approximate expression for  $\Pi_{\text{el}}$  (cf. ref 23):

$$\Pi_{\text{el}} \cong 2RT \Gamma \quad (4)$$

The most reasonable theoretical models of ionized monolayers, which assume a partial binding of counterions in the Stern–Helmholtz layer, were presented in refs 24 and 25. The ionization could be approximately accounted for by using the equation of state and adsorption isotherm derived in ref 23 and allowing for a counterion binding in the Stern–Helmholtz layer by assuming that the degree of binding does not depend on the adsorption. Therefore, the Frumkin equations in ionized adsorption layers read

$$\Pi = -\frac{2RT}{\omega} [\ln(1 - \theta) - \varphi\theta + a\theta^2] \quad (5)$$

$$b[c(c + c_2)]^{1/2} f = \frac{\theta^{1+2\varphi}}{1 - \theta} \exp(-2a\theta) \quad (6)$$

where  $\varphi$  is the fraction of free (unbound) surface active ions at the surface. For  $\varphi = 0$ , eqs 5–6 are identical to eqs 1–2. Usually, the fraction of unbound surface-active ions is low and does not exceed 10–30% of the amount of adsorbed ions.<sup>1,21</sup>

The data obtained for C<sub>n</sub>TAB solutions of different hydrocarbon chain lengths were analyzed in the framework of eqs 1–2 and eqs 5–6. It appeared that the introduction of the additional parameter  $\varphi$  does not improve the agreement between the experimental  $\Pi(c)$  data and the theoretically calculated values. Setting  $\varphi \neq 0$  the best fit of the theoretically calculated values to the experimental data requires essentially higher values of the coefficient  $a$  and slightly lower values of the molar area of surfactants  $\omega$  than for  $\varphi = 0$ . In other words, in the model which assumes the electroneutrality of the surface layer (eqs 1–2), the contribution to the surface pressure caused by the repulsion of equally charged ions is not accounted for. To achieve the best possible fit between the experimental data and theoretical values, this contribution should be compensated by a decrease of the intermolecular interaction coefficient  $a$ . It follows from the calculations that the variation in  $\varphi$  does not significantly change the high-frequency limit of the elasticity  $E_0 = d\Pi/d \ln \Gamma$ . As is with  $\varphi = 0$ , a monotonic increase of  $E_0$  versus  $c$  (or  $\Pi$ ) is predicted, in contrast to experimental data.<sup>2,5,15</sup> Therefore, in the analysis presented below we do not use the model given by eqs 5–6, because this model does not add any essential features to that described by eqs 1–2.

Another model used here to analyze the adsorption behavior of C<sub>n</sub>TAB solutions is based on the assumption of an intrinsic compressibility of adsorbed molecules (CM model), provided by the reorientation of their hydrocarbon chains. In brief, the model considers changes in the tilt angle or in the adsorption of the packed surface layer because of an increased surface pressure.<sup>20</sup> As was shown in ref 19, a finite compressibility  $\epsilon$

has little effect on the adsorption isotherm while it changes the dilational elasticity significantly. Taking into account that the surfactants dissociate into two ions, and introducing the expressions for the mean activity of ions in the solution as derived in ref 20 (involving rigorous expressions for the surface layer nonideality of enthalpy and entropy), one obtains the following equation of state and adsorption isotherm:

$$\Pi = -\frac{RT}{\omega_0} [\ln(1 - \theta) + (1 - 1/n)\theta + a\theta^2], \quad (7)$$

$$b[c(c + c_2)]^{1/2} f = \frac{\theta}{n(1 - \theta)^n} \exp[-2an\theta]. \quad (8)$$

Here,  $\omega$  is the molar area of the ionic surfactant,  $\omega_0$  is the molar area of a solvent molecule, and  $n = \omega/2\omega_0$ . As was done in our previous work,<sup>18–20</sup> it can be assumed that the molar area of the surfactant  $\omega$  in eqs 7 and 8 depends linearly on the surface pressure:

$$\omega = 2\omega_0(1 - \epsilon\Pi) \quad (9)$$

where the proportionality factor  $\epsilon$  is the relative two-dimensional compressibility of the surfactant molecules in the surface layer. Together with eq 9, one can express  $\theta$  and  $n$  in eqs 7 and 8 as

$$\theta = \Gamma\omega = 2\Gamma\omega_0(1 - \epsilon\Pi), \quad (10)$$

$$n = 1 - \epsilon\Pi. \quad (11)$$

It is interesting to compare the limiting elasticity for the Frumkin model 1–2 with that obtained from model 7–8. For  $\theta \rightarrow 1$  it follows from eq 1 that  $E_0 \rightarrow \infty$ , in contradiction to all experimental results available, while the model 7–8 yields a finite value of  $E_0$ , namely,

$$E_0 = \frac{1 - \epsilon\Pi}{\epsilon} \quad (12)$$

In particular, for  $\epsilon = 0.005$ – $0.01$  m mN<sup>-1</sup> which is usual for common surfactants<sup>16,19</sup> at a surface pressure of  $\Pi = 40$  mN m<sup>-1</sup>, it follows from eq 12 that  $E_0 = 160$ – $60$  mN m<sup>-1</sup>, in qualitative agreement with experimental data.

### 3. Experimental Section

**Materials and Cleaning Procedure.** The cationic alkyl trimethylammonium bromides C<sub>i</sub>TAB with  $i = 12, 14$ , and  $16$  were purchased from Aldrich. All surfactants were purified by recrystallizing them three times with pure acetone to which traces of ethanol were added. The solutions were prepared with Milli-Q water. All glassware was cleaned with deconex from Borer Chemie (as a replacement for chromic sulfuric acid) and rinsed thoroughly with water before use.

**Surface Tension Measurements.** The static surface tensions were measured at 22 °C by the Du Noüy ring method, using a Krüss K10ST tensiometer. Dynamic surface tensions were measured at 22 °C by maximum bubble pressure tensimetry, using the MPT2 tensiometer from LAUDA.

### 4. Results and Discussion

**Static Surface Tension.** In Figures 1–3, the equilibrium surface tensions  $\gamma$  for aqueous solutions of C<sub>12</sub>TAB, C<sub>14</sub>TAB, and C<sub>16</sub>TAB, respectively, are plotted versus the surfactant

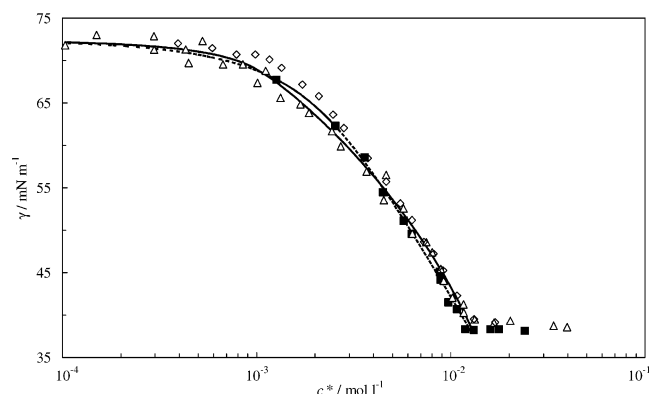


**Figure 1.** The dependence of equilibrium surface tension  $\gamma$  for the  $C_{12}$ TAB solutions on the activity  $c^*$ : (◇), data ref 1; (Δ), data ref 13; (■), our data; theoretical curves calculated from the Frumkin (dashed line) and CM model (full line) using the parameters of Tables 1 and 2.

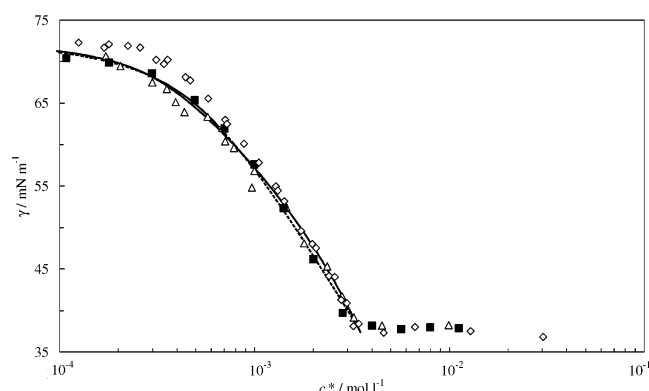


**Figure 2.** The dependence of equilibrium surface tension  $\gamma$  for the  $C_{14}$ TAB solutions on the activity  $c^*$ : (◇), data ref 1; (Δ), data ref 5; (■), our data; theoretical curves are denoted as in Figure 1.

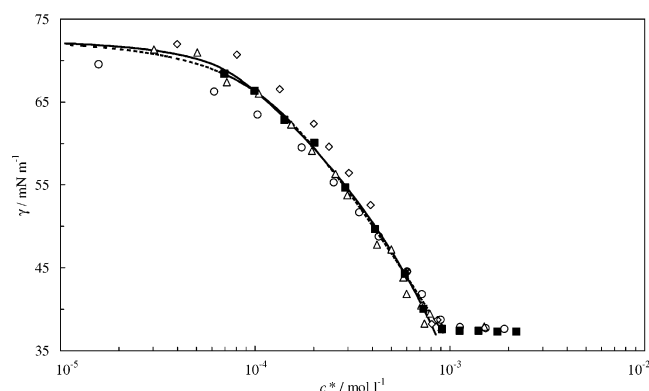


**Figure 3.** The dependence of equilibrium surface tension  $\gamma$  for the  $C_{16}$ TAB solutions on the activity  $c^*$ : (◇), data ref 1; (Δ), data ref 5; (○), data ref 4; (■), our data; theoretical curves are denoted as in Figure 1.

activity  $c^*$ . As no salt was added, that is,  $c_2 = 0$ , one obtains  $c^* = f(c(c + c_2)^{1/2}) = fc$  where  $f$  can be calculated according to eq 3.

The figures show our results and data reported in the literature.<sup>1,4,5,13</sup> The agreement between the experimental data obtained in different studies is within acceptable limits. The theoretical curves in Figures 1–3 were calculated on the basis of the data obtained in the study at hand using two models: the Frumkin model given by eqs 1–2 and the CM model given by eqs 7–8 which assume the intrinsic compressibility of molecules in the surface layer. The model parameters are listed in Tables 1 and 2, respectively. It is seen that both models reproduce the experimental  $\Pi(c^*)$  curves excellently, and

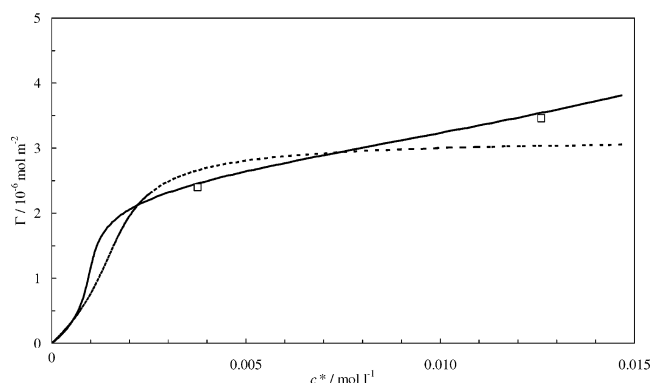


**Figure 4.** The dependence of the  $C_{12}$ TAB adsorption  $\Gamma$  on the activity  $c^*$ : (□), experimental data ref 11; theoretical curves calculated from the Frumkin (dashed line) and CM model (full line) using the parameters of Tables 1 and 2.

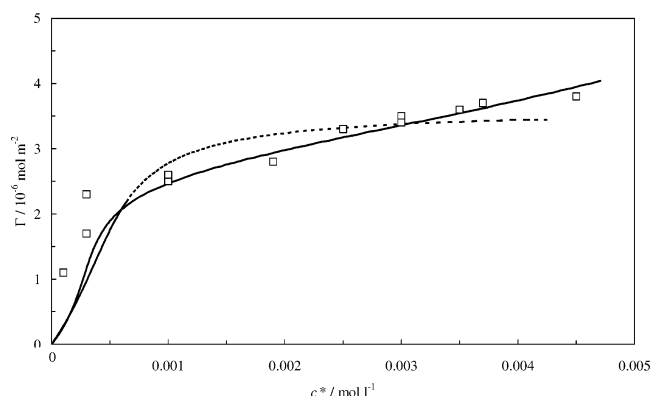


**Figure 5.** The dependence of the  $C_{14}$ TAB adsorption  $\Gamma$  on the activity  $c^*$ : (□), experimental data ref 12; theoretical curves are denoted as in Figure 4.

**TABLE 1: Parameters of the Frumkin Model**

$C_n$ TAB	$\omega_0/10^5 \text{ m}^2 \text{ mol}^{-1}$	$a$	$b/l \text{ mol}^{-1}$
$n = 12$	2.58	0.96	174
$n = 14$	2.76	0.99	716
$n = 16$	2.92	1.0	3112

**TABLE 2: Parameters of the CM Model (Compressibility of Surfactant Molecules)**

$C_n$ TAB	$\omega_0/10^5 \text{ m}^2 \text{ mol}^{-1}$	$a$	$b/l \text{ mol}^{-1}$	$\epsilon/m \text{ mN}^{-1}$
$n = 12$	2.20	1.40	242	0.012
$n = 14$	2.12	1.30	962	0.010
$n = 16$	2.08	1.58	3095	0.011

therefore neither of these models can be preferred solely on the basis of these results.

**Surfactant Adsorption.** With the parameters obtained from the Frumkin and the CM model (see Tables 1 and 2), the surfactant adsorption  $\Gamma$  can be calculated as a function of the surfactant activity  $c^*$ . The respective results for  $C_{12}$ TAB and  $C_{14}$ TAB are shown in Figures 4 and 5 together with adsorption values that have been measured using neutron reflection.<sup>11,12</sup> The calculations for  $C_{16}$ TAB lead to the same general trend (data are not shown). Experimental data, however, are not available so far.

As can be seen in Figures 4 and 5, the CM model describes the experimental data much better than the Frumkin model. While the Frumkin model shows an asymptotic behavior of the  $\Gamma(c^*)$  curve, which is nearly parallel to the  $x$ -axes at concentrations near the CMC, the CM model predicts an almost linear increase of the adsorption in this concentration range, in agreement with the neutron reflection experiments.

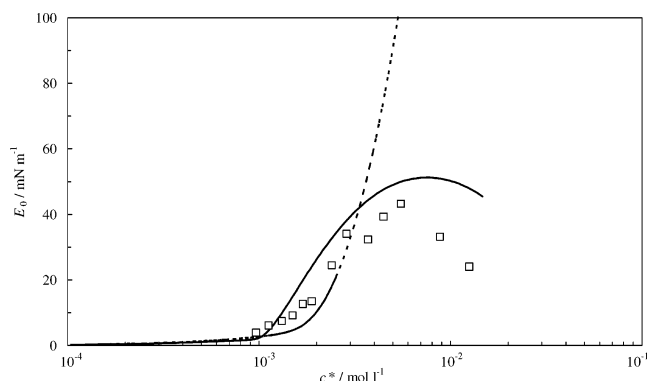


**Figure 6.** The dependence of the limiting elasticity  $E_0$  of the  $C_{12}$ TAB adsorption layer on the activity  $c^*$ : ( $\square$ ), experimental data ref 13; theoretical curves calculated from the Frumkin (dashed line) and CM model (full line) using the parameters of Tables 1 and 2.

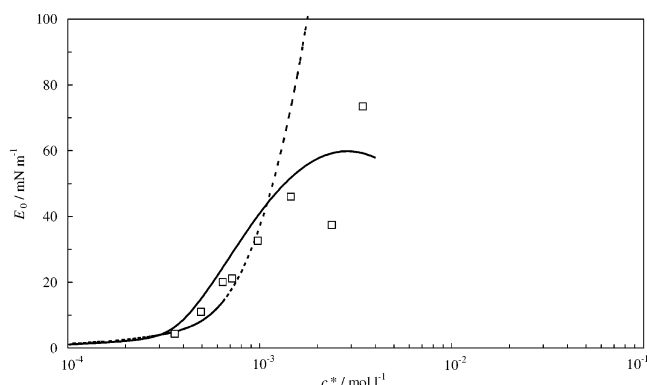


**Figure 7.** The dependence of the limiting elasticity  $E_0$  of the  $C_{14}$ TAB adsorption layer on the activity  $c^*$ : ( $\square$ ), experimental data ref 5; theoretical curves are denoted as in Figure 6.

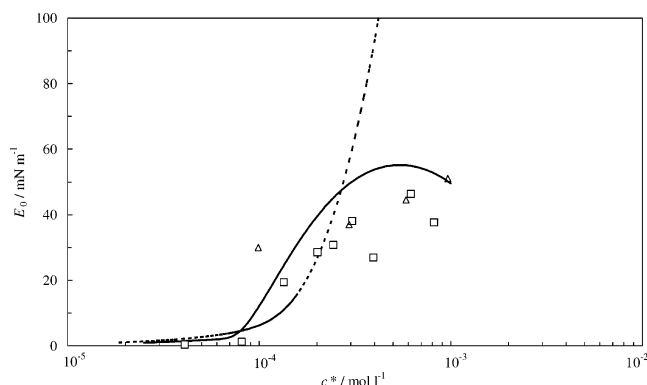


**Figure 8.** The same as in Figure 7 for  $C_{16}$ TAB, ( $\Delta$ ), experimental data ref 30.

**Surface Elasticities.** The advantages of the CM model become much more evident in Figures 6–8, where the experimental limiting elasticities for the  $C_{12}$ TAB,  $C_{14}$ TAB, and  $C_{16}$ TAB adsorption layers<sup>5,13</sup> are compared with the results predicted by the two models. The  $E_0$  values for  $C_{12}$ TAB were estimated in ref 13 via extrapolation to the limiting oscillation frequency. The  $E_0$  values for  $C_{14}$ TAB and  $C_{16}$ TAB, however, were calculated from the real (r) and imaginary (i) parts of the complex elasticity  $E$  according to<sup>19</sup>

$$E_0 = \frac{E_r^2 + E_i^2}{E_r - E_i} \quad (13)$$

Equation 13 follows from the theory developed by Lucassen and van den Tempel<sup>26,27</sup> and the required data are given in ref

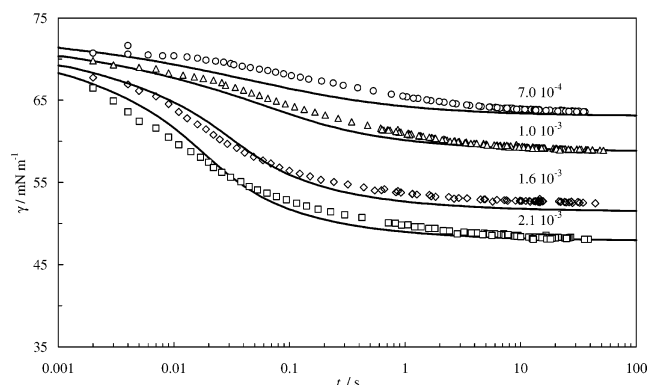


**Figure 9.** The dependence of the surface tension  $\gamma$  for  $C_{14}$ TAB on the effective time  $t$ ; curves denoted according to the  $C_{14}$ TAB concentration in  $\text{mol l}^{-1}$ ; theoretical curves calculated from eqs 1, 2, and 14.

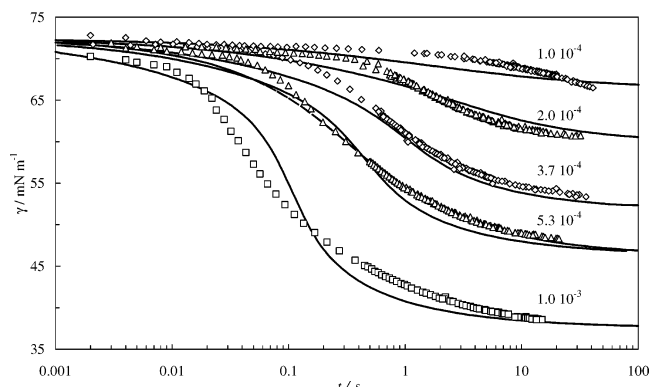


**Figure 10.** The same as in Figure 9 for  $C_{16}$ TAB; dashed theoretical curve for  $c = 5.3 \times 10^{-4} \text{ mol l}^{-1}$  calculated from eqs 7, 8, and 14.

5 for a fixed frequency of 800 Hz. As the imaginary part  $E_i$  of the elasticity at 800 Hz is much lower than the real part  $E_r$ , the values of  $E_0$  calculated from eq 13 were close to the values of  $E_r$ . Comparing the theoretical dependencies plotted in Figures 6–8 with the experimental data, one can clearly see that the CM model is superior to the Frumkin model.

The  $E_0(c^*)$  curves calculated for the CM model pass a maximum, in contrast to the Frumkin model. This maximum is shifted toward lower concentrations with increasing surface activity of the surfactant, that is, from  $7.5 \times 10^{-3} \text{ mol l}^{-1}$  for  $C_{12}$ TAB over  $3.0 \times 10^{-3} \text{ mol l}^{-1}$  for  $C_{14}$ TAB down to  $5.5 \times 10^{-4} \text{ mol l}^{-1}$  for  $C_{16}$ TAB. In any case, the given approach allows us to describe the experimental data in a quite satisfactory way compared to the results obtained on the basis of the Frumkin model. It is not only the overall appearance but also the absolute elasticity values that are described by the more sophisticated CM model. The discrepancies seen in Figures 6–8 are not automatically a weakness of the model. Having in mind how demanding surface rheological measurements are, these discrepancies can simply be due to the large experimental error.

**Dynamic Surface Tensions.** In addition to the description of the static surface tension, the adsorption, and the surface elasticity, the new CM model also describes the dynamic surface tension adequately. The experimental dynamic surface tensions for aqueous solutions of  $C_{14}$ TAB and  $C_{16}$ TAB are shown in Figures 9 and 10 as a function of the so-called effective (adsorption) time  $t$ .<sup>28</sup> The corresponding theoretical  $\gamma(t)$  curves are also shown. They were calculated from the Ward and Tordai equation:<sup>29</sup>

$$\Gamma(t) = 2f\sqrt{\frac{D}{\pi}}[c_0\sqrt{t} - \int_0^t c(0, t-t')d\sqrt{t'}] \quad (14)$$



where  $c_0$  is the bulk concentration,  $t$  is the time,  $t'$  is a dummy integration variable, and  $D$  is the diffusion coefficient. As boundary condition, the adsorption isotherm eq 2 was used and the diffusion coefficients were set equal to  $D = 2 \cdot 10^{-10} \text{ m}^2 \text{ s}^{-1}$  and  $1 \cdot 10^{-10} \text{ m}^2 \text{ s}^{-1}$  for  $\text{C}_{14}\text{TAB}$  and  $\text{C}_{16}\text{TAB}$ , respectively.

One can see that the calculations describe the experimental curves  $\gamma(t)$  quite satisfactorily. However, the values of the diffusion coefficients are substantially lower than the theoretical estimates for these surfactants, which are about  $5 \cdot 10^{-10} \text{ m}^2 \text{ s}^{-1}$ .<sup>7,13</sup> If the adsorption isotherm of the CM model, that is, eq 8 instead of eq 2, is used as the boundary condition for eq 14, only minor changes in the dynamic curves are observed. Thus, the diffusion coefficients remain almost the same, as it is shown in Figure 10 for one concentration. It can be argued that the adsorption of  $\text{C}_n\text{TAB}$  at the water/air interface is not only governed by diffusion, that is, that adsorption barriers have to be taken into account.

## 5. Conclusions

In the study at hand, experimental static surface tensions, surfactant adsorption, limiting surface elasticities, and dynamic surface tensions of the cationic alkyl trimethylammonium bromides  $\text{C}_{12}\text{TAB}$ ,  $\text{C}_{14}\text{TAB}$ , and  $\text{C}_{16}\text{TAB}$  are presented and analyzed with a new theoretical model, the so-called CM model. Literature data on static surface tension isotherms were completed by a series of dynamic surface tensions. All experimental data were analyzed by two different theoretical adsorption models, namely, the classical Frumkin and the newly developed CM model. In the latter, an intrinsic compressibility of the surfactant monolayer is taken into account. This model was recently applied to analyze respective experimental data of nonionic surfactants. That this model can be extended to the description of ionic surfactants was clearly shown in the present study. Whereas with the Frumkin model essential properties such as the static and the dynamic surface tensions can be described satisfactorily, the description of the surfactant adsorption is of lower quality and the description of the limiting surface elasticity  $E_0$  is not possible at all. In contrast to that, all features characteristic of the adsorption layers formed by each  $\text{C}_n\text{TAB}$  homologue can be reproduced satisfactorily by a single set of parameters defined for the theoretical CM model. It is above all the  $E_0$  values of the surfactant monolayer that we are now able to calculate. Thus, the assumption of an intrinsic compressibility of the  $\text{C}_n\text{TAB}$  molecules at the surface is an important issue and should be included in future considerations dealing with the rheological interfacial behavior.

**Acknowledgment.** We thank J. Schlarmann for measuring the static and dynamic surface tensions. C.S. is indebted to the FCI, the Ministerium für Wissenschaft und Forschung des Landes NRW, and the DFG for financial support.

## References and Notes

- (1) Bergeron, V. *Langmuir* **1997**, *13*, 3474.
- (2) Langevin, D.; Argillier, J.-F. *Macromolecules* **1996**, *29*, 7412.
- (3) Lu, J. R.; Thomas, R. K.; Aveyard, R.; Binks, B. P.; Cooper, P.; Fletcher, P. D. I.; Sokolowski, A.; Penfold, J. *J. Phys. Chem.* **1992**, *96*, 10971.
- (4) Shchukin, E. D.; Markina, Z. N.; Zadymova, N. M. *Prog. Colloid Polym. Sci.* **1983**, *68*, 90.
- (5) Monroy, F.; Giermanska Khan, J.; Langevin, D. *Colloids Surf., A* **1998**, *143*, 51.
- (6) Li, B.; Geeraerts, G.; Joos, P. *Colloids Surf., A* **1994**, *88*, 251.
- (7) Geeraerts, G.; Joos, P.; Ville, F. *Colloids Surf., A* **1995**, *95*, 281.
- (8) Hutchison, J.; Klennerman, D.; Manning-Benson, S.; Bain, C. *Langmuir* **1999**, *15*, 7530.
- (9) Lu, J. R.; Simister, E. A.; Thomas, R. K.; Penfold, J. *Prog. Colloid Polym. Sci.* **1993**, *93*, 92.
- (10) Lu, J. R.; Hromadova, M.; Simister, E. A.; Thomas, R. K.; Penfold, J. *J. Phys. Chem.* **1994**, *98*, 11519.
- (11) Lytle, D. J.; Lu, J. R.; Su, T. J.; Thomas, R. K.; Penfold, J. *Langmuir* **1995**, *11*, 1001.
- (12) Simister, E. A.; Lee, E. M.; Thomas, R. K.; Penfold, J. *J. Phys. Chem.* **1992**, *96*, 1373.
- (13) Stenvot, C.; Langevin, D. *Langmuir* **1988**, *4*, 1179.
- (14) Bell, G. R.; Manning-Benson, S.; Bain, C. D. *J. Phys. Chem. B* **1998**, *102*, 218.
- (15) Knock, M. M.; Bell, G. R.; Hill, E. K.; Turner, H. J.; Bain, C. *Langmuir* **2000**, *16*, 2857.
- (16) Fainerman, V. B.; Miller, R.; Kovalchuk, V. I. *Langmuir* **2002**, *18*, 7748.
- (17) Rusanov, A. I. *Mendeleev Commun.* **2002**, *1*, 218.
- (18) Fainerman, V. B.; Miller, R.; Kovalchuk, V. I. *J. Phys. Chem. B* **2003**, *107*, 6119.
- (19) Kovalchuk, V. I.; Loglio, G.; Fainerman, V. B.; Miller, R. *J. Colloid Interface Sci.* **2004**, *270*, 34.
- (20) Fainerman, V. B.; Kovalchuk, V. I.; Aksenenko, E. V.; Michel, M.; Leser, M. E.; Miller, R. *J. Phys. Chem. B* **2004**, *108*, 13700.
- (21) Fainerman, V. B.; Lucassen-Reynders, E. H. *Adv. Colloid Interface Sci.* **2002**, *96*, 295.
- (22) Robinson, R. A.; Stokes, R. H. *Electrolyte Solutions*; Butterworths: London, 1965.
- (23) Fainerman, V. B. *Colloids Surf.* **1991**, *57*, 249.
- (24) Danov, K. D.; Vlahovska, P. M.; Kralchevsky, P. A.; Mehreteab, A.; Broze, G. *Colloids Surf., A* **1999**, *156*, 389.
- (25) Kralchevsky, P. A.; Danov, K. D.; Broze, G.; Mehreteab, A. *Langmuir* **1999**, *15*, 2351.
- (26) Lucassen, J.; van den Tempel, M. *Chem. Eng. Sci.* **1972**, *27*, 1283.
- (27) Lucassen, J.; van den Tempel, M. *J. Colloid Interface Sci.* **1972**, *41*, 491.
- (28) Miller, R.; Joos, P.; Fainerman, V. B. *Adv. Colloid Interface Sci.* **1994**, *49*, 249.
- (29) Ward, A. F. H.; Tordai, L. *J. Chem. Phys.* **1946**, *14*, 543.
- (30) Fruhner, H.; Wantke, K.-D.; Lunkenheimer, K. *Colloid Surf., A* **2000**, *162*, 193.